# OIL SHALE RETORTING KINETICS

P. H. Wallman, P. W. Tamm, B. G. Spars

Chevron Research Company
576 Standard Avenue
Richmond, California  94802

Several aboveground oil shale retorting processes are charac-
terized by rapid heating followed by retorting at essentially iso-
thermal conditions.  The objective of this study is to investigate the
retorting kinetics applicable to processes characterized both by rapid
heating of relatively small particles and by rapid sweeping of the
produced hydrocarbon vapors out of the retort.  Rather surprisingly,
accurate kinetics for these conditions are not available in the
literature.

Several previous investigators have taken an isothermal approach
but have failed to eliminate significant heatup effects in the mea-
sured kinetics.  The important investigation by Hubbard and
Robinson (1) is in this category.  Attempts were made to correct the
Hubbard and Robinson data for the heatup effects by Braun and
Rothman (2) and Johnson et al. (3).  Allred (4) took new isothermal
data with increased accuracy, but his results also suffered from
interfering heat-transfer dynamics.  Weitkamp and Gutberlet (5) used
both isothermal and nonisothermal techniques but covered only low
temperatures and presented no kinetic model.

A frequent characteristic of past investigations is excessive
complexity of the proposed kinetic models.  The works of Fausett
et al. (6) and Johnson et al. (3) belong in this category.  A goal of
the present investigation is to keep the model as simple as possible.

One previous investigation that deserves special attention is
that by the Lawrence Livermore Laboratory (LLL) described in Campbell
et al. (7) and Campbell et al. (8).  The LLL group determined retort-
ing kinetics by both isothermal and nonisothermal experiments with
reasonable agreement between the two approaches.  However, the LLL
work was directed toward in-situ retorting where heating rates are
inherently low.  Low heating rates were found to decrease the oil
yield below Fischer Assay levels by increasing coke formation.  For
small particles, the detrimental effect of slow heating could be
eliminated by sweeping the sample with an inert gas implying that the
coking was associated with holdup in a liquid state.  Such coking is
not of importance in the present investigation where the sample is
well swept, and heatup rates are three orders of magnitude higher than
typical in-situ rates.

The LLL kinetic model predicts that the maximum achievable oil
yield is that of Fischer Assay and that the coke associated with
Fischer Assay is stoichiometrically related to the kerogen.  This
assumption may be appropriate for in-situ retorting, but it is not
applicable to the present conditions where oil yields higher than
Fischer Assay are measured.  Consequently, another objective of this
work is to extend the kinetics of oil production beyond the Fischer
Assay limit.

Experimental Technique - A bench-scale fluidized bed reactor shown in Figure 1 was used to retort small samples of oil shale particles. The glass reactor held a bed of inert solids such as glass beads or sand that was continuously fluidized by a controlled flow of helium or any other gas. A weighed sample of shale in an amount no greater than 2% of the bed was dropped into the preheated reactor, producing a negligible drop in bed temperature. Heat transfer in the fluidized bed was very rapid, and the volatile products were rapidly swept out by the fluidizing gas. The vapor residence time in the reactor was typically 3 seconds. A small sample stream was diverted to a flame ionization detector (FID in Figure 1). The FID produced a signal proportional to the concentration of total hydrocarbon. Heteroatom content of evolved products was assumed constant with time. Since the hydrocarbon concentration dropped to very low levels at the end of the retorting reaction, the sensitivity of the detector had to be increased by at least a factor of ten as the retorting progressed. This increased sensitivity made it possible to record the full product-evolution curve including the long "tail" which contains information on the kinetics at high conversion levels. Attempts were made to use the FID for quantitative determination of volatile hydrocarbon yields, but the results were of insufficient accuracy. The area under the curve did, however, give an approximate yield which was used as an experimental check.

Oil and gas yields were obtained from another branch of the apparatus shown in Figure 1. The oil was condensed in a cold trap, and the gases were collected in a gas cylinder by liquid displacement. The amount of oil was determined gravimetrically, and the amount of hydrocarbon gas was determined from the total volume of gas collected and the gas composition. The oil was recovered by $CS_2$ extraction and subjected to GC analysis, standardized against n-paraffins. Finally, to close the hydrocarbon balance, the entire bed consisting of inert particles and retorted shale was recovered and its hydrocarbon content determined.

The oil collection trap shown in Figure 1 proved to be a critical part of the apparatus. The product oil tends to form a stable aerosol making it difficult to collect. This problem can be overcome by a trap design where the condensation occurs under a steep thermal gradient. The inside wall of the cold trap was kept at 300°F while the opposite wall was in contact with a bath at 5°F. A thermally induced outward radial flow promoted film condensation on the cold wall. Interestingly, this design eliminated aerosol formations when using helium as the fluidizing gas; but with heavier gases such as argon, nitrogen, and even methane, aerosol formation still occurred. The cause of this effect was not investigated, but it could be related to differences in conductivity between the gases. The selected bath temperature of 5°F proved practical because no butanes condensed, and only a small portion of light oil ($C_5$–$C_7$) was lost to the gas. This light oil was accounted for by use of the gas analysis.

Another area of experimental difficulty was gas analysis. At low temperatures requiring long reaction times, large amounts of helium were necessary; and the hydrocarbon products were in very low concentration. This difficulty was overcome by recycling the gas back into the fluidized bed and thereby allowing the hydrocarbon concentration

to build up.  Some oil vapor was undoubtedly recycled increasing the possibility of thermal cracking.

The shale samples used in this work were obtained by screening from a single bulk sample of Colorado oil shale (Anvil Point Mine, courtesy of Development Engineering Incorporated and the U.S. Department of Energy).  The Fischer Assay oil yield was 10.5% (27.5 gallons/ton) for the larger particles and somewhat lower for the finer size cuts, for example, 10.15% for 100 μm particles.  These and all subsequent percentages reported in this paper are on a weight basis.

Yield Results - Experiments were conducted to determine the effect of oil shale particle size on product yields at 930°F.  The yields obtained for particles of six different sizes are compared with Fischer Assay yields in Figure 2.  It is apparent that oil yields higher than Fischer Assay are obtained for small particles; whereas large particles produce Fischer Assay yield.  The incremental oil produced from small particles is balanced by a decreased coke make while the gas make remains constant.  The oil yield appears to have a limit at about 110% Fischer Assay, but this may be entirely due to the limited range of particle sizes investigated.  It is possible that the oil yield would increase further for, say, 10-μ or 1-μ particles.  However, particles of this size could not be studied in the apparatus of this work.

Not only do smaller particles produce more oil, but there is also a change in the oil composition.  The concentration of $C_{29}+$ in the product oil is shown in Figure 3.  Increased oil yields are accompanied by increased heavy ends.  Hence, the conclusion is that the incremental oil obtained from small particles is of higher molecular weight.

The effect of retorting temperature on the yields obtained from 0.4-mm particles and the accompanying change in oil composition are shown in Figures 4 and 5.  The important findings here are that coke yield is unaffected by retorting temperature and that oil yield is increased due to decreased gas make at the lower temperatures.  This second finding suggests decreased cracking since Figure 5 shows that a lighter oil product is obtained at the higher temperatures.  It will also be noted that the data set shown in Figure 4 has some "extra" cracking in comparison with the data of Figure 2.  This is due to the fact that the results of Figure 4 were obtained in the recycle gas mode  where recycling of a small portion of the oil occurred.  In general, the gas make was found to be very sensitive to equipment conditions such as the temperature of the product line leading to the condenser.

Kinetic Results - The kinetic complement to the yield results discussed above was obtained from the FID response curve.  Integration of this curve gave the fractional conversion.  Figure 6 shows the results of the particle-size effect experiments plotted as the logarithm of the fraction unconverted hydrocarbon versus time (the term hydrocarbon is used here to denote organic matter).  It appears that the results can be described by a pair of first-order processes since the curves can be approximated by two straight-line segments. By comparing the slopes of the two segments, the rates of the two

72

processes are found to differ by a factor of ten. This is an important finding with consequences for the retorting model to be proposed in a subsequent section.

The small differences between the initial segments of the kinetic curves is due to differences in heatup time for the different particle sizes. However, heatup time is relatively unimportant even for the 3-mm particles because the straight-line segment extrapolates to only 15 seconds on the time axis. This "experimental" heatup time is about what one would calculate using a heat transfer coefficient of 500 $W/m^2$ °C.

An important feature of the results shown in Figure 6 is that the slope of the latter segment of the curve changes for particles of different size. The process corresponding to this segment appears to be slower for the small particles than for the large ones. This unexpected characteristic is at first surprising. It is, however, a consequence of the different yields for different particle sizes shown in Figure 2. The yield differences do not enter the kinetic results of Figure 6 because the ordinate is normalized by the total hydrocarbon evolved (this type of plot is required for determination of the rate constants).

The kinetic and yield data are combined in Figure 7 for the 0.4-mm and 3-mm particles. This figure shows that the hydrocarbon evolution is essentially independent of particle size up to 100% Fisher Asay oil yield. At this level the oil production stops for large particles, whereas it continues for small particles at a reduced rate.

The effect of temperature on the retorting kinetics is shown in Figure 8 for the 1-mm particles. Both processes respond to temperature but the fast one more so than the slow one.

Table I

Retorting Rate Expressions

Light Hydrocarbon Production:

$$\text{Rate} = f_1 \cdot k_1 \cdot C_o \cdot e^{-k_1 t}$$

$$\text{Amount} = f_1 \cdot k_1 \cdot C_o \cdot (1 - e^{-k_1 t})$$

Primary Heavy Oil Production:

$$\text{Rate} = f_2 \cdot k_2 \cdot C_o \cdot e^{-(k_2 + k_c) t}$$

$$\text{Amount} = f_2 \frac{k_2}{k_2 + k_c} C_o \cdot [1 - e^{-(k_2 + k_c) t}]$$

Intraparticle Coke Production:

$$\text{Rate} = f_2 \cdot f_c \cdot k_c \cdot C_o \cdot e^{-(k_2 + k_c) t}$$

$$\text{Amount} = f_2 \cdot f_c \frac{k_c}{k_2 + k_c} C_o \cdot [1 - e^{-(k_2 + k_c) t}]$$

Retorting Model - The combined kinetic and yield data can be correlated with the retorting model shown in Figure 9. Here kerogen decomposes into a "light" hydrocarbon product and a heavy intermediate product, "bitumen." The light product is largely a vapor at retorting conditions and is, therefore, produced rapidly without significant secondary reactions. The bitumen, on the other hand, is of high boiling range and remains in the particle for significant periods of time. It becomes subject to two competing processes: (1) heavy oil production and (2) intraparticle (liquid-phase) coking. The released heavy oil is further subjected to thermal cracking in the vapor phase surrounding the particles.

First-order rate expressions are proposed in Table I for the three principal steps: light hydrocarbon production (equals kerogen decomposition), primary heavy oil production, and coking.

The model accounts for the dramatic change in oil production rate which is observed. The fast initial rate is governed by the rate constant $k_1$ (first order in kerogen concentration). The latter slow rate is governed by the sum of the two bitumen reactions, which are assumed first order in the intraparticle bitumen concentration and have rate constants $k_2$ and $k_c$. At the temperatures of interest, $k_1$ is much greater than $k_2 + k_c$ so that the first step of the reaction goes virtually to completion before there is any appreciable conversion of the bitumen.

Table II

Light Hydrocarbon Fraction, $f_1$

| Particle Size, mm | Light Hydrocarbon Total Volatile-Hydrocarbon Yield, % of Kerogen | Yield, % of Total Volatile Hydrocarbon | Light Hydrocarbon Yield, % of Kerogen |
|---|---|---|---|
| 3 | 68.8 | 90 | 61.9 |
| 2 | 70.0 | 87 | 60.9 |
| 1 | 71.1 | 87 | 61.9 |
| 0.4 | 74.4 | 83 | 61.8 |
| | | Avg = 61.6 | |

The "stoichiometry" of the kerogen decomposition reaction is given by the product fractions $f_1$, $f_2$, and $f_w$ in Figure 9. The ($H_2O$, CO, $CO_2$) fraction was set equal to that of Fischer Assay because the fraction of water in the liquid product could not be easily determined in the yield experiments. The light hydrocarbon fraction, $f_1$, was determined by a combination of the yield and the kinetic data. The light hydrocarbon yield as a fraction of total volatile hydrocarbon was obtained by extrapolating the slow reaction segments of Figure 6 to zero time and reading the fractions off the ordinate. The results are shown in Table II. The values of $f_1$ obtained for the four particle sizes are sufficiently constant to justify an average value of

74

61.6%. The stoichiometry is independent of temperature as shown in Figure 8 where all the slow reactor segments extrapolate back to approximately the same point on the ordinate, namely 87% light hydrocarbon. The bitumen fraction, $f_2$, in Figure 9 is obtained by difference and equals 24%. Hence, $f_2$ is constant with both particle size and temperature at least in the range of 900-1000°F. Finally, a ratio between coke and gas in the coking reaction of 80:20 was set on the assumption that the gas yield at 800°F in Figure 4 is the result of coking alone. Campbell et al. (8) used essentially the same coke-gas ratio for a similar reaction in their reaction sequence.

A second source of gas is vapor-phase cracking of the heavy oil released from the particle. Cracking of the light hydrocarbon fraction is also possible; but because it occurs to a lesser extent, it has been assumed to be zero. The kinetics of the cracking reaction lie outside the scope of the present investigation, but this important reaction has been studied by Burnham and Taylor (9).

A third source of gas is the initial decomposition of kerogen itself. The contribution of each step cannot be determined with the FID detector because it cannot distinguish between gas and oil.

The kerogen decomposition rate constant, $k_1$, and the bitumen disappearance rate constant ($k_2 + k_c$) are obtained directly as the slopes of the two straight-line segments of Figures 6 and 8 (and similar graphs for the other particle sizes). Figure 10 shows the temperature dependence of these rate constants. It is also seen that $k_1$ is independent of particle size. This implies that there is no significant resistance to the transport of light hydrocarbons from the interior of the particle into the bulk of the carrier gas. This condition is a consequence of the high vapor pressure of the light hydrocarbon fraction. Because of the rapid transport out of the particle, this fraction has no possibility to coke. The bitumen, on the other hand, is viewed as a high boiling liquid which can undergo intraparticle coking. The particle size dependence of ($k_2 + k_c$) in Figure 10 suggests that a diffusional resistance may be important in the heavy oil production step. Also, the activation energy for the reactions governing bitumen disappearance is only 22.6 kcal/mole as compared to 43.6 kcal/mole for the kerogen decomposition reaction.

In order to determine $k_2$ and $k_c$ individually, the kinetically determined values for the sum ($k_2 + k_c$) must be used in consort with the expression for the coke yield $0.8 \cdot f_2 \cdot k_c/(k_2+k_c)$. The calculated values of the ratio $k_c/(k_2+k_c)$ together with the kinetically obtained values of ($k_2 + k_c$) are given in the Appendix. The resulting $k_2$ and $k_c$ values show some interesting characteristics: $k_2$ is independent of particle size whereas $k_c$ is proportional to particle size. Both have the same temperature dependence because the coke yield is constant with temperature. The temperature dependence and the particle size dependence of $k_c$ are shown explicitly in Table III.

Table III

Rate Constants (Min.$^{-1}$)

Kerogen Decomposition:
$$k_1 = 5.78 \cdot 10^{12} \exp \left( - \frac{43.6 \text{ kcal/mole}}{R \cdot T} \right)$$

Heavy Oil Production:
$$k_2 = 1.8 \cdot 10^5 \exp \left( - \frac{22.6 \text{ kcal/mole}}{R \cdot T} \right)$$

Coking:
$$k_c = A_c \cdot \exp \left( - \frac{22.6 \text{ kcal/mole}}{R \cdot T} \right)$$

| where $A_c$ | Particle Size, mm |
|---|---|
| $18 \cdot 10^5$ | 3 |
| $9 \cdot 10^5$ | 2 |
| $5 \cdot 10^5$ | 1 |
| $3 \cdot 10^5$ | 0.4 |

Discussion – As part of this investigation, models different from the one proposed here were considered. One such model of particular appeal is similar in structure to the one given in Figure 9 but with a pure diffusion process for the heavy oil production. However, this alternative model is incompatible with some experimental findings: It predicts lower coke concentrations on the surface of the particle than in the interior, whereas microprobe results indicate a uniform coke distribution. Further, this diffusion model predicts zero coke yield for infinitely small particles, whereas the limited amount of data available for small particle sizes suggest a leveling-off of the coke yield below a particle size of 0.4 mm.

The approach to Fischer Assay yield structure with increasing particle size is accounted for in the proposed model by complete coking of the bitumen fraction. The model predicts a coke yield of 19% of the kerogen when the bitumen is completely coked well within Fischer Assay range. Therefore, fluid bed and Fischer Assay retorting give different yields for small particles only. The interpretation of this is that in a Fischer Assay retort small particles produce the same amount of coke as large particles because there is no sweep gas to facilitate oil removal from the small particles. The fluid bed retorting experiments have shown that additional oil can indeed be produced from small particles.

The proposed model can be compared with both the model of Allred (4) and that of Campbell et al. (8). Allred's model does not have the feature of competing parallel reactions that is essential to the retorting model proposed here. It does, however, have the intermediate product bitumen which reaches a maximum level almost identical to the one in this work. Allred postulates that all kerogen decomposes into bitumen, whereas bitumen in the present work is the remainder of the kerogen after the light hydrocarbon fraction has been stripped off.

There are some interesting similarities and contrasts between the present model and the Lawrence Livermore Laboratory (LLL) model of Campbell et al.(8) The activation energy of the initial decomposition

is similar in both models, 48–54 kcal/mole in the case of LLL and 44 kcal/mole here. Bitumen is treated merely as an intermediate in the kerogen decomposition by LLL; whereas, here it is one of several decomposition products. Coking steps are included in both models, but the material involved is different. The coking kinetics accounted for by LLL only apply to the light hydrocarbon of the present model, and this coking reaction does not occur here because of the high heating rate and the sweep gas. The coking considered in the present model involves the intermediate bitumen product and the coking rate depends on particle size. Small particles produce less coking and; consequently, oil yields higher than Fischer Assay.

Both Allred (4) and Weithamp and Gutberlet (5) observed the slow oil production regime. Calculating a rate constant for this slow production regime at 856°F from the results of the latter investigators gives a value of 0.12 min.$^{-1}$ identical to ($k_2$ + $k_c$) of this work.

A practical implication of the results of this work is that Fischer Assay yield is probably a practical upper limit for any retorting process. This work has shown that a very small particle size increases oil yield and decreases coke yield, but long reaction times are necessary. Low coke yields may not be desirable from overall heat balance considerations if the coke is to be used as an energy source for the process. Lowering the temperature also increases oil yield but at the expense of the gas yield and with the requirement of long reaction times. Very small particle sizes are uneconomical because of high grinding costs, and low processing temperatures are uneconomical because of the large reactor volumes required.

This work has added to the understanding of the very complex phenomena occurring during oil shale retorting. The simple retorting model will be useful in modeling product yields from retorting processes handling small size particles at high retorting rates.

References

1.  Hubbard, A. B., and Robinson, W. E., "A Thermal Decomposition Study of Colorado Oil Shale," Report of Investigation 4744, Bureau of Mines, Washington, D.C., 1950.

2.  Braun, R. L., and Rothman, A. J., Fuel, 54, 129 (1975).

3.  Johnson, W. F.; Walton, D. K.; Keller, H. H.; and Couch, E. J., "Quarterly of the Colorado School of Mines," 70, No. 3, 237 (1975).

4.  Allred, V. D., Chem. Eng. Progr., 62, No. 8, 55 (1966).

5.  Weitkamp, A. W., and Gutberlet, L. C., Ind. Eng. Chem. Process Des. Develop., 9, No. 3, 386 (1970).

6.  Fausett, D. W.; George, J. H.; and Carpenter, H. C., "Second-Order Effects in the Kinetics of Oil Shale Pyrolysis," Report of Investigation 7889, Bureau of Mines, Washington, D.C., 1974.

7. Campbell, J. H.; Koskinas, G. H.; and Stout, N. D., "The Kinetics of Decomposition of Colorado Oil Shale: I. Oil Generation," Report UCRL-52089 Prepared for the U.S. Energy Research and Development Administration, Lawrence Livermore Laboratory, June 1976.

8. Campbell, J. H.; Koskinas, G. H.; Coburn, T. T.; and Stout, N. D., "Oil Shale Retorting: The Effects of Particle Size and Heating Rate on Oil Evolution and Intraparticle Oil Degradation," Report UCRL-52256 Prepared for the U.S. Energy Research and Development Administration, Lawrence Livermore Laboratory, April 1977.

9. Burnham, A. K., and Taylor, J. R., "Shale Oil Cracking. 1. Kinetics," Report UCID-18284 Prepared for the U.S. Energy Research and Development Administration, Lawrence Livermore Laboratory, October 1979.

## A P P E N D I X

### HEAVY OIL PRODUCTION AND COKING RATE CONSTANTS, $k_2$ AND $k_c$ (RATE CONSTANTS IN MIN.$^{-1}$, COKE YIELDS IN % KEROGEN)

| Particle Size, mm | | 900°F | 930°F | 950°F | 980°F | 1000°F |
|---|---|---|---|---|---|---|
| 3 | $k_2 + k_c$ | | 0.887 | | 1.04 | |
| | Coke Yield | 16.8 | | | | |
| | $k_c/(k_2 + k_c)$ | 0.875 | | | | |
| | $k_c$ | | 0.776 | | 0.908 | |
| | $k_2$ | | 0.111 | | 0.130 | |
| 2 | $k_2 + k_c$ | | 0.442 | | 0.545 | |
| | Coke Yield | 15.6 | | | | |
| | $k_c/(k_2 + k_c)$ | 0.813 | | | | |
| | $k_c$ | | 0.359 | | 0.443 | |
| | $k_2$ | | 0.083 | | 0.102 | |
| 1 | $k_2 + k_c$ | 0.186 | 0.292 | 0.367 | 0.378 | 0.587 |
| | Coke Yield | 14.5 | | | | |
| | $k_c/(k_2 + k_c)$ | 0.755 | | | | |
| | $k_c$ | 0.140 | 0.220 | 0.277 | 0.285 | 0.443 |
| | $k_2$ | 0.046 | 0.072 | 0.090 | 0.093 | 0.144 |
| 0.4 | $k_2 + k_c$ | | 0.197 | | 0.296 | |
| | Coke Yield | 11.2 | | | | |
| | $k_c/(k_2 + k_c)$ | 0.583 | | | | |
| | $k_c$ | | 0.115 | | 0.173 | |
| | $k_2$ | | 0.082 | | 0.123 | |

:vlh,kab

# FIGURE 1
## FLUID-BED REACTOR SYSTEM FOR OIL SHALE RETORTING
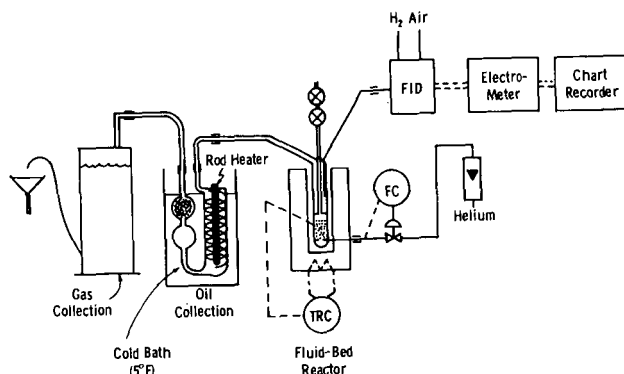


# FIGURE 2
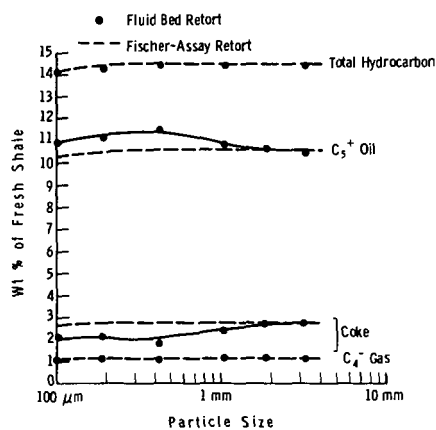## PARTICLE SIZE EFFECT ON HYDROCARBON YIELDS AT 930°F



# FIGURE 3
## CORRELATION BETWEEN OIL YIELD AND OIL COMPOSITION
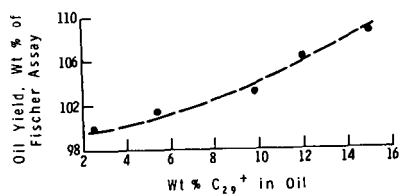


# FIGURE 4
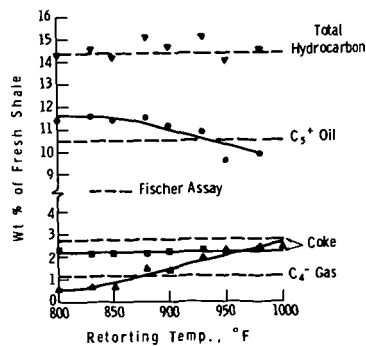## TEMPERATURE EFFECT ON HYDROCARBON YIELDS FOR 0.4 mm PARTICLES

FIGURE 5

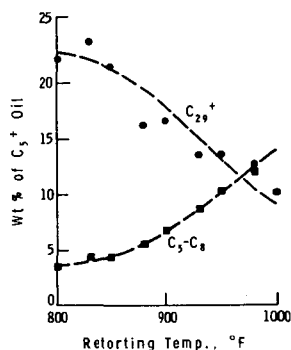OIL COMPOSITION AS A
FUNCTION OF
RETORTING TEMPERATURE

FIGURE 6
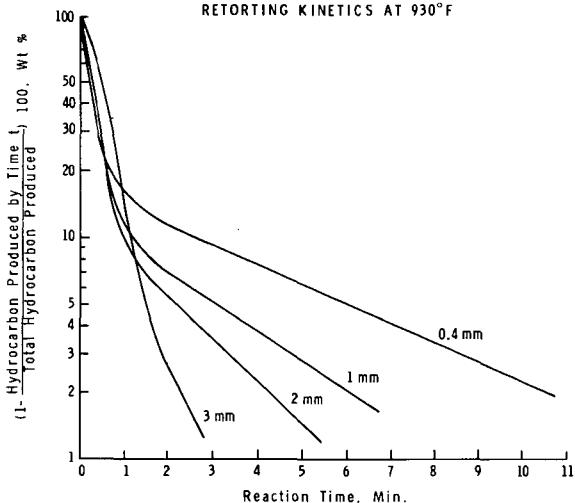PARTICLE SIZE EFFECT ON
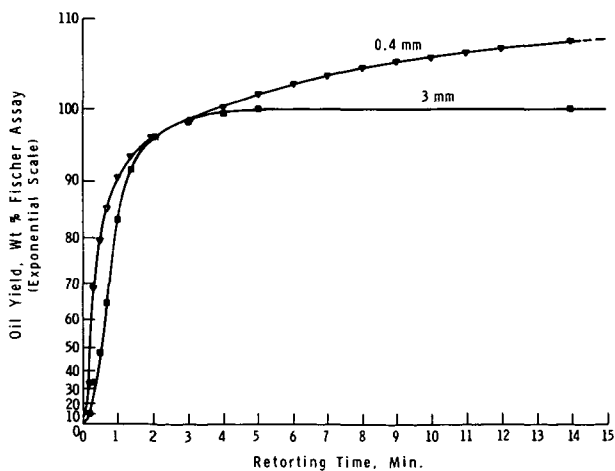RETORTING KINETICS AT 930°F

FIGURE 7

OIL PRODUCTION KINETICS AT 930°F
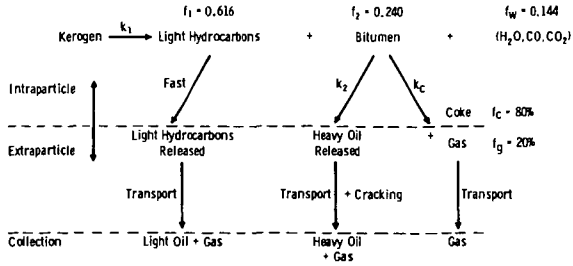


80

FIGURE 9
PROPOSED RETORTING MODEL
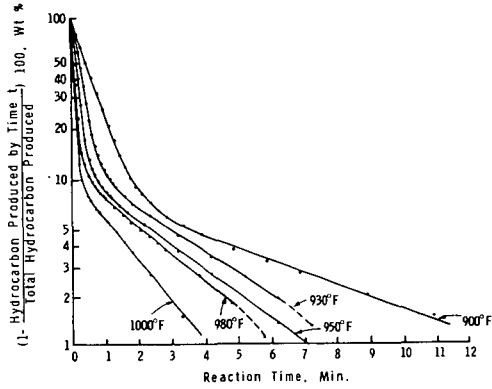


FIGURE 8
TEMPERATURE EFFECT ON RETORTING
KINETICS FOR 1 mm PARTICLES



FIGURE 10
RETORTING RATE CONSTANTS

81